

# Effect of angular-momentum dissipation and fluctuation on energy coherence lengths and time evolution in the dissipative collision $^{28}\text{Si} + ^{48}\text{Ti}$

S. Yu. Kun<sup>a,b,1</sup>, W. Nörenberg<sup>a,c</sup> and M. Papa<sup>d</sup>

<sup>a</sup> *Gesellschaft für Schwerionenforschung (GSI), Pf. 110552, W-6100 Darmstadt 11, FRG*

<sup>b</sup> *Centre for Nonlinear Studies, Physics Department, WITS University, Johannesburg, South Africa*

<sup>c</sup> *Institut für Kernphysik, TH Darmstadt, W-6100 Darmstadt, FRG*

<sup>d</sup> *Laboratorio Nazionale del Sud, Istituto Nazionale di Fisica Nucleare, via S. Sofia, I-95123 Catania, Italy*

Received 17 September 1992

We analyze the energy autocorrelation functions and the energy coherence lengths in the strongly dissipative collision  $^{28}\text{Si}(E_{\text{lab}} = 130 \text{ MeV}) + ^{48}\text{Ti}$  for  $Z = 11$  and 12 reaction fragments. It is found that in order to obtain a good fit of both the energy-averaged angular distributions and the angular dependence of the energy coherence lengths one has to take into account (i) the dissipation and fluctuation of the relative angular momentum of the dinucleus and (ii) the contribution from direct (fast) reactions in addition to the statistical (relatively slow) interaction processes. The established angular dependence is a direct consequence of the angular-momentum dissipation-fluctuation effects on the time-space evolution of the intermediate dinucleus.

## 1. Introduction

The study of fluctuations in excitation functions of dissipative heavy-ion collisions (DHIC) [1–6] provides us with direct informations on the time evolution of the collision process. Indeed, the energy autocorrelation function (EAF) of the fluctuating cross-section is expressed by the Fourier transform of the time-space distribution of the intermediate dinuclear system. As a result the time characteristics, such as average rotation velocity, average life-time and angular dispersion of the rotating decaying dinucleus, can be extracted by means of the analysis of the cross-section fluctuations in DHIC [7–12].

The excitation functions of the differential cross-sections contain informations about *time-space evolution* of the rotating dinucleus, which is related to the relative angular momentum. The time evolution of the relative angular momentum is characterized by dissipation and fluctuation which conveniently are calculated from a Fokker-Planck equation [13–15].

The main consequences of this angular-momentum diffusion process on the EAF have been studied recently [16]. Remarkably large effects have been found on both the time power spectrum (TPS) of the decaying dinucleus, and, as a result, on the EAF of fluctuations.

A different derivation [12,17] of the TPS has been given in terms of a multistep  $S$ -matrix representation which also allows to model the transport of relative angular momentum into intrinsic spin of the dinucleus. These results support the expression for the time-space distribution of the intermediate dinucleus [16] calculated in the framework of the diffusion model [13–15].

In ref. [16] we illustrated the method for the strongly dissipative collision  $^{28}\text{Si}(E_{\text{lab}} = 130 \text{ MeV}) + ^{48}\text{Ti}$  without considering the complete set of data. This letter is devoted to a complete and more realistic description of the experimental cross-sections. This includes the angular dependence of the energy coherence lengths for  $Z = 11$  and 12 fragments.

<sup>1</sup> Present address: Theoretical Physics Department, RSPHYS, ANU, GPO Box 4, Canberra, 2601 ACT, Australia.

## 2. Time power spectrum in the framework of the angular-momentum diffusion approach

The basic element for the fluctuation analysis is the expression for the TPS which accounts for the diffusion of relative angular momentum of the decaying dinucleus [16],

$$\begin{aligned} \tilde{P}(t, \theta) = & H(t) (\sin \theta)^{-1} [4\pi a + 2\pi \sigma_{\Psi\Psi}^2(t)]^{-1/2} \\ & \times \exp(-\Gamma t/\hbar) \\ & \times \left[ \sum_{n=-\infty}^{\infty} \exp\left(-\frac{(\Phi + \theta + 2\pi n - \langle \Psi \rangle_t)^2}{4a + 2\sigma_{\Psi\Psi}^2(t)}\right) \right. \\ & \left. + \sum_{m=-\infty}^{\infty} \exp\left(-\frac{(\Phi - \theta + 2\pi m - \langle \Psi \rangle_t)^2}{4a + 2\sigma_{\Psi\Psi}^2(t)}\right) \right]. \end{aligned} \quad (1)$$

Here, the decay constant of the dinucleus is denoted by  $\Gamma$ . The mean deflection function  $\Phi$  results from an angular-momentum expansion of the potential phase shifts in the entrance and exit channels. It determines the average orientation of the dinucleus at the time ( $t=0$ ) of its formation, which is expressed by the Heaviside function  $H(t)$ . The time-independent variance  $2a$  of the orientation of the dinucleus is given by

$$2a = \frac{1}{2} (d^{-2} + \dot{\Phi}^2 d^2), \quad (2)$$

where  $\dot{\Phi}$  is the derivative of the deflection function with respect to  $l$  taken at the initial average angular momentum  $L$ , and  $d$  is the size of the reaction  $l$ -window. The sum over  $n$  includes contributions resulting from multiple rotations of the dinucleus. The average rotation angle of the dinucleus  $\langle \Psi \rangle_t$  is determined according to the diffusion equation by [13–15]

$$\langle \Psi \rangle_t = \omega_{st} t + (\omega - \omega_{st}) \tau_{ang} [1 - \exp(-t/\tau_{ang})], \quad (3)$$

where  $\omega_{st} = L_{st}/\mathcal{I}_{rel}$  and  $L_{st} = L(1 - \mathcal{I}_{int}/\mathcal{I}_{tot})$  denote the sticking values of the angular velocity and the relative angular momentum, respectively. Here,  $\mathcal{I}_{int}$  is the sum  $\mathcal{I}_1 + \mathcal{I}_2$  of the intrinsic moments of inertia of the interacting nuclei,  $\mathcal{I}_{rel}$  is the relative moment of inertia of the dinucleus and  $\mathcal{I}_{tot} = \mathcal{I}_{int} + \mathcal{I}_{rel}$  is the total moment of inertia.

The time-dependent component of the angular dispersion of the rotating dinucleus results from the

angular-momentum diffusion and is given by

$$\begin{aligned} \sigma_{\Psi\Psi}^2(t) = & \langle (\Psi - \langle \Psi \rangle_t)^2 \rangle_t \\ = & T \tau_{ang} \frac{\mathcal{I}_{int}}{\mathcal{I}_{rel} \mathcal{I}_{tot}} [2t - 3\tau_{ang} + 4\tau_{ang} \exp(-t/\tau_{ang}) \\ & - \tau_{ang} \exp(-2t/\tau_{ang})]. \end{aligned} \quad (4)$$

Here,  $T$  denotes the dinucleus temperature. The relaxation time  $\tau_{ang}$  for angular-momentum dissipation is given by

$$\tau_{ang} = (T/D_{MM}) \mathcal{I}_{int} \mathcal{I}_{rel} / \mathcal{I}_{tot}, \quad (5)$$

where  $D_{MM}$  is the angular-momentum diffusion coefficient.

The TPS (1) transforms to that without angular-momentum dissipation by putting  $\langle \Psi \rangle_t = \omega t$  and  $\sigma_{\Psi\Psi}^2(t) = 0$  for  $\tau_{ang} \gg \hbar/\Gamma$ . This limit means that the dinucleus decays before a sensible amount of relative angular momentum is dissipated. The TPSs with and without angular-momentum dissipation differ in two respects. Firstly, the power spectrum exhibits a decrease in angular velocity due to the dissipation of relative angular momentum, while the TPS without angular-momentum dissipation corresponds to rotation with a constant angular velocity. Secondly, due to the diffusion of the relative angular momentum, the angular dispersion of dinuclear orientation increases with time [cf. eq. (4)]. In other words, the dissipation and fluctuation of relative angular momentum yield damping of the rotation velocity of the dinucleus and delocalization in orientation.

Eq. (1) for the TPS, which includes the effects of angular-momentum dissipation, represents the basis for calculating the EAF of the fluctuating cross-section. Physically, the angular-momentum dissipation modifies the *energy autocorrelation*, because it introduces *new time dependences* in the collision process. The new time scales are the angular-momentum relaxation time and the rotation period for the sticking value of the relative angular velocity.

## 3. Analysis of cross-section fluctuations in $^{28}\text{Si} + ^{48}\text{Ti}$

We employ the above formulation to study the effects of angular-momentum dissipation in the strongly dissipative collision  $^{28}\text{Si}(E_{lab} = 130 \text{ MeV}) + ^{48}\text{Ti}$  in the exit channels  $Z = 11$  and  $12$  [3–5]. The angular

distributions (fig. 1) for both fragments are very similar and show strong focussing near the grazing angle  $\theta_{gr}=50^\circ$ , while outside of  $\theta_{gr}$  they are supposedly given by an isotropic background. Accordingly we assume the contributions from two reaction mechanisms: a quasielastic mechanism with a decay constant  $\Gamma=\Gamma_{qe}\gg\hbar\omega$ , and a statistical one with  $\Gamma=\Gamma_{stat}<\hbar\omega$  which generates fluctuations in the cross-section.

The similarity of the angular distributions in fig. 1 is not surprising because of the neighbourhood of the charges  $Z=11$  and  $12$  of the reaction fragments. In addition, the experimental data on the angular dependence of the energy coherence lengths are very similar (see fig. 2). Therefore, we fit the data for  $Z=11$  and  $12$  using the same set of parameters.

For the energy-averaged cross-section we have

$$\langle\sigma(E,\theta)\rangle=(\sin\theta)^{-1}[\sigma_{qe}(E,\theta)+\langle\sigma_{stat}(E,\theta)\rangle] \quad (6)$$

with

$$\begin{aligned} \sigma_{qe}(E,\theta) &= \int_0^\infty dt \tilde{P}_{qe}(t,\theta) \\ &= A \exp[-(\theta-\Phi)^2/4a_{qe}] \end{aligned} \quad (7)$$

and

$$\langle\sigma_{stat}(E,\theta)\rangle = \int_0^\infty dt \tilde{P}_{stat}(t,\theta) = K, \quad (8)$$

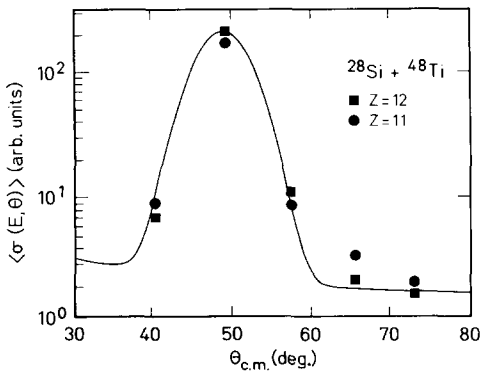


Fig. 1. Angular distributions of the  $Z=11$  and  $12$  fragments from the collision  $^{28}\text{Si} + ^{48}\text{Ti}$  at  $E_{lab}=130$  MeV. The curve represents a fit in accordance to eqs. (6)–(8). The data are from refs. [4,5].

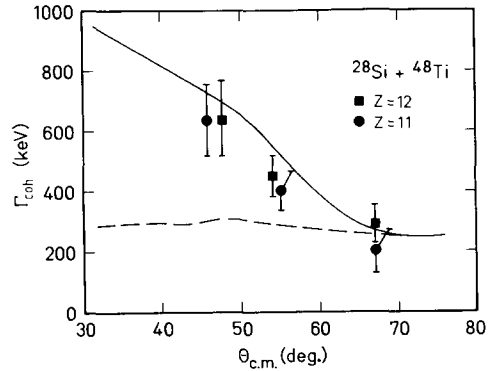


Fig. 2. Angular dependence of the energy coherence lengths (coherence energies)  $\Gamma_{coh}$  for the  $Z=11$  and  $12$  fragments in the collision  $^{28}\text{Si} + ^{48}\text{Ti}$  at  $E_{lab}=130$  MeV. The solid curve is calculated from eqs. (1), (9) and (10) with angular-momentum dissipation. The dashed line is calculated without angular-momentum dissipation. Parameters are given in the text. The data are from refs. [3–5].

where  $\tilde{P}_{qe}$  and  $\tilde{P}_{stat}$  are given by eq. (1). In the derivation of  $\sigma_{qe}(E,\theta)$  through  $\tilde{P}_{qe}(t,\theta)$  we have replaced  $\exp(-\Gamma_{qe}t/\hbar)$  by  $\delta(t)$  because of  $\hbar\omega\ll\Gamma_{qe}$ . The constants  $A$ ,  $K$ ,  $a_{qe}=\frac{1}{4}(1/d_{qe}^2+\dot{\Phi}_{qe}^2d_{qe}^2)$  and  $\Phi$  are determined by a fit to the experimental data on the angular distribution. We obtain  $A=200$  and  $K=2$  (both in arbitrary units),  $a_{qe}=0.0016$  and  $\Phi=50^\circ$ . Putting  $\dot{\Phi}_{qe}=0$  we have  $d_{qe}=12.5$ . For the  $l$ -window of the dissipative contribution we assume  $d_{stat}=d_{qe}=12.5$ . To obtain a rough estimate for the derivative of the deflection function for the statistical process we use a simple estimate  $\dot{\Phi}_{stat}=\pi/L=0.0628$  where the value  $L=50$  [3] was used. This yields  $a_{stat}=0.15$ .

In order to fit the experimental coherence lengths (coherence energies)  $\Gamma_{coh}$  (which were defined in refs. [3–5] as the minimal widths at half maxima of the EAF  $C(\epsilon,\theta)$ ) in the  $^{28}\text{Si} + ^{48}\text{Ti}$  dissipative reaction for  $Z=11$  and  $12$ , we use the expression

$$C(\epsilon,\theta)=|\zeta(\epsilon,\theta)|^2+2\sigma_{qe}(\theta)\text{Re}\zeta(\epsilon,\theta) \quad (9)$$

with  $\zeta(\epsilon,\theta)$  expressed by the TPS (1) as

$$\zeta(\epsilon,\theta)\sim\int_{-\infty}^{\infty} dt \exp(iet/\hbar)\tilde{P}_{stat}(t,\theta). \quad (10)$$

The solid curve in fig. 2 is obtained from eqs. (1), (9) and (10) with the decay constant  $\Gamma_{stat}=270$  keV for the dinucleus. A quasiclassical estimate yields

$\hbar\omega = 1$  MeV [3], while  $\omega_{st}/\omega = 0.71$ , where  $\omega_{st}$  is the angular velocity which corresponds to the sticking angular momentum. We take the temperature to be  $T = 1.5$  MeV which corresponds approximately to 30 MeV excitation energy above the yrast line. We estimate the diffusion coefficient from eq. (3.4) of ref. [14]. Then, taking into account the dependence of  $D_{MM}$  on  $A_1 + A_2$ , we obtain  $D_{MM}(\text{Si} + \text{Ti}) \approx \frac{1}{3} D_{MM}(\text{Kr} + \text{Er})$ , while  $D_{MM}(\text{Kr} + \text{Er})$  was found, on the basis of the analysis of data [13], to be equal to  $D_{MM}(\text{Kr} + \text{Er})/\hbar^2 = 10^{23} \text{ s}^{-1}$ . Accordingly, taking  $D_{MM}(\text{Si} + \text{Ti})/\hbar^2 = 0.33 \times 10^{23} \text{ s}^{-1}$  and using eq. (3) of ref. [13], we have  $\tau_{ang} = 6 \times 10^{-22} \text{ s}$  which corresponds to  $\theta_{ang} = \tau_{ang}\omega = 0.92$  rad. All other parameters are the same as determined before to reproduce the angular distributions in fig. 1.

In fig. 3, the EAFs for  $\theta = 40^\circ, 50^\circ$  and  $60^\circ$  are shown. In order to interpret the strong variation in  $C(\epsilon, \theta)$  and  $\Gamma_{coh}$  in the vicinity of  $\theta = \Phi = 50^\circ$  we refer to the corresponding TPSs in fig. 4. We observe that the decrease of  $\Gamma_{coh}$  with increasing  $\theta$  reflects the transition from strongly overlapping near- and far-side contributions in time for  $\theta < \Phi = 50^\circ$  to the contribution mostly from the far side for  $\theta > \Phi = 50^\circ$ . Thus, the angular dependence of  $\Gamma_{coh}$  is the direct consequence of the high sensitivity of the EAF of the fluctuating cross-section to the shape of the TPS, and

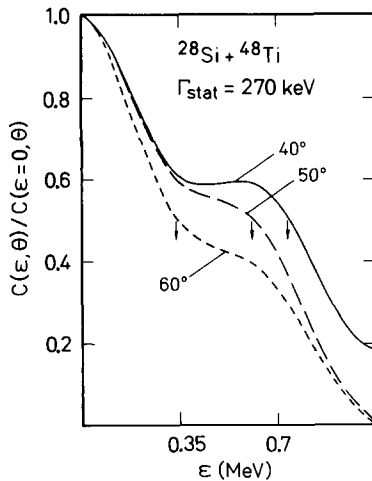


Fig. 3. Energy autocorrelation functions  $C(\epsilon, \theta)$  for  $\theta = 40^\circ, 50^\circ, 60^\circ$  calculated from eqs. (1), (9) and (10). Parameters are given in the text. The arrows indicate the coherence energies.

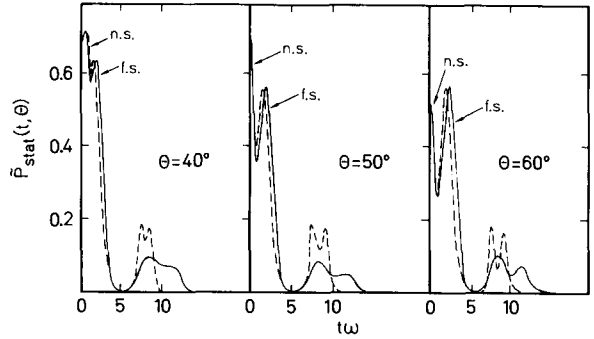


Fig. 4. The time power spectra for  $\theta = 40^\circ, 50^\circ, 60^\circ$ . Solid lines are calculated with angular-momentum dissipation. Dashed lines are calculated without angular-momentum dissipation. Parameters are given in the text. The notations n.s. and f.s. indicate near- and far-side contributions.

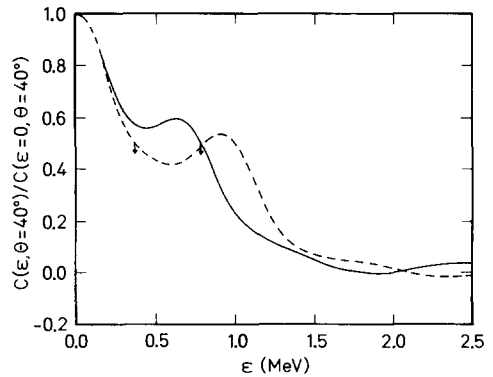


Fig. 5. Energy autocorrelation functions  $C(\epsilon, \theta = 40^\circ)$  with (solid line) and without (dashed line) angular-momentum dissipation. Parameters are given in the text. The arrows indicate the coherence energies.

hence to the detailed *time-space evolution* of the collision process.

In fig. 2 we also display the angular dependence of the energy coherence length calculated without angular-momentum dissipation. The difference in the behaviour of the *energy autocorrelation characteristics* appears due to the *different time-space evolutions* of the dinucleus (see fig. 4) with and without angular-momentum dissipation.

The sensitivity of the EAF to angular-momentum dissipation is further illustrated in fig. 5, where the solid and dashed lines are with and without angular-momentum dissipation, respectively. The inclusion of angular-momentum dissipation increases the en-

ergy coherence length  $\Gamma_{\text{coh}}$  of fluctuations by more than a factor two, from 360 keV to 780 keV.

Note that a good fit of the angular dependence of  $\Gamma_{\text{coh}}$  in  $^{28}\text{Si} + ^{48}\text{Ti}$  was already obtained in ref. [8]. However, there it was necessary to use an angular velocity considerably smaller (280 keV) than the realistic one of 1 MeV [3]. Furthermore, the strong focussing in the angular distributions could not be reproduced in ref. [8], because the contribution of direct reactions was not taken into account. In the present work we have reproduced both the angular dependence of  $\Gamma_{\text{coh}}$  and the strong focussing in  $\langle \sigma(E, \theta) \rangle$  using a realistic value for the angular velocity  $\hbar\omega = 1$  MeV. As mentioned in ref. [8] we attribute this to the incorporation of both the angular-momentum dissipation and the contribution from direct processes.

#### 4. Conclusion

We have demonstrated that the analysis of the *energy structures in the excitation functions of DHIC* is a sensitive tool to study the *time-space evolution of the intermediate dinucleus*. In particular, the analysis of the energy autocorrelation clearly shows remarkable effects from angular-momentum dissipation in the  $^{28}\text{Si} + ^{48}\text{Ti}$  collision. Indeed, the angular-momentum dissipation changes the TPS of the intermediate dinucleus. This is the reason why the EAF, as the Fourier transform of the TPS, is changed, accordingly.

Physically, the energy autocorrelation is sensitive to angular-momentum dissipation because it changes the time evolution of the collision process introducing *new time scales* such as angular-momentum relaxation time and the rotation period for the sticking angular velocity.

Such details of the time evolution of the collision process are not available from the analysis of the energy averaged angular distributions. Indeed these are *time-integrated* reaction characteristics. In particular, the angular distributions in fig. 1 are the same with and without angular-momentum dissipation. Thus we conclude that the study of fluctuations in excitation functions of DHIC, in addition to energy averaged values, provides us with new information on the reaction mechanisms and their time-space evolution.

#### Acknowledgement

This work was initiated during the visit of one of us (S.K.) at GSI, Darmstadt and his stay at MPI für Kernphysik, Heidelberg on Humboldt Fellowship and MPI Fellowship.

#### References

- [1] A. De Rosa, G. Inglima, V. Russo, M. Sandoli, G. Fortuna, G. Montagnoli, C. Signorini, A.M. Stefanini, G. Cardella, G. Pappalardo and F. Rizzo, Phys. Lett. B 160 (1985) 239.
- [2] T. Suomijärvi, B. Berthier, R. Lucas, M.C. Mermaz, J.P. Coffin, G. Guillaume, B. Heusch, F. Jundt and F. Rami, Phys. Rev. C 36 (1987) 181.
- [3] A. De Rosa, G. Inglima, V. Russo, M. Sandoli, G. Fortuna, G. Montagnoli, C. Signorini, A.M. Stefanini, G. Cardella, G. Pappalardo and F. Rizzo, Phys. Rev. C 37 (1988) 1042.
- [4] G. Pappalardo, Nucl. Phys. A 488 (1988) 395c.
- [5] A. De Rosa, G. Inglima, E. Rosato, M. Sandoli, G. Cardella, M. Papa, G. Pappalardo, F. Rizzo, G. Fortuna, G. Montagnoli, A.M. Stefanini, A. Tivelli and C. Signorini, Phys. Rev. C 40 (1989) 627.
- [6] A. De Rosa, E. Fioretto, G. Inglima, M. Romoli, M. Sandoli, G. Cardella, M. Papa, F. Rizzo, D.R. Napoli, A.M. Stefanini and C. Signorini, Phys. Rev. C 44 (1991) 747.
- [7] S.Yu. Kun, Proc. 5th Intern. Conf. on Nuclear reaction mechanisms (Varenna, June 1988), ed. E. Gadioli, p. 353.
- [8] G. Cardella, M. Papa, G. Pappalardo, F. Rizzo, A. De Rosa, G. Inglima and M. Sandoli, Z. Phys. A 332 (1989) 195.
- [9] A. De Rosa, E. Fioretto, G. Inglima, M. Romoli, M. Sandoli, R. Setola, G. Cardella, M. Papa, G. Pappalardo, F. Rizzo, Q. Wang, G. Montagnoli, G.F. Segato, C. Signorini and A.M. Stefanini, Z. Phys. A 336 (1990) 387.
- [10] S.Yu. Kun, Phys. Lett. B 257 (1991) 247.
- [11] G. Pappalardo and M. Papa, Proc. Workshop on Direct multistep nuclear reactions (Faure, October 1991) (World Scientific, Singapore).
- [12] S.Yu. Kun, in: Proc. Workshop on Direct multistep nuclear reactions (Faure, October 1991) (World Scientific, Singapore).
- [13] G. Wolschin and W. Nörenberg, Phys. Rev. Lett. 41 (1978) 691.
- [14] S. Ayik, G. Wolschin and W. Nörenberg, Z. Phys. A 286 (1978) 271.
- [15] W. Nörenberg and H.A. Weidenmüller, Introduction to the theory of heavy-ion collisions, Lecture Notes in Physics, Vol. 51 (Springer, Berlin, 1980); A. Gobbi and W. Nörenberg, in: Heavy ion collisions, ed. R. Bock, Vol. 2 (North-Holland, Amsterdam, 1980).
- [16] S.Yu. Kun and W. Nörenberg, Z. Phys. A 343 (1992) 215.
- [17] S.Yu. Kun and H.A. Weidenmüller, Proc. 6th Intern. Conf. on Nuclear reaction mechanisms (Varenna, June 1991), ed. E. Gadioli, p. 259.